

# INFLUENCE OF RAINFALL SPATIAL VARIABILITY ON RUNOFF SIMULATION IN HILLY IRRIGATION AREAS

CHEN, J. L.<sup>1</sup> – LUO, W. B.<sup>1\*</sup> – WANG, W. J.<sup>2</sup> – YU, L.<sup>1</sup> – LI, Y. L.<sup>1</sup> – ZOU, Z. K.<sup>1</sup> – HAN, X. D.<sup>3\*</sup> – HUANG, S. Z.<sup>4</sup>

<sup>1</sup>*Agricultural Water Conservancy Department, Yangtze River Scientific Research Institute, Wuhan 430010, China*

<sup>2</sup>*Hanjiang Bureau of Hydrology and Water Resources Survey, Changjiang Water Resources Commission, Xiangyang 441022, China*

<sup>3</sup>*State Key Laboratory of Water Resources Engineering and Management, Wuhan University, Wuhan 430072, China*

<sup>4</sup>*College of Resources and Environment, Yangtze University, Wuhan 430100, China*

*\*Corresponding authors*

*e-mail/phone: luowenbing2005\_0@126.com/+86-134-0718-3483;*

*hanxudong@whu.edu.cn/+86-150-7100-2290*

(Received 27<sup>th</sup> Feb 2024; accepted 13<sup>th</sup> Jun 2024)

**Abstract.** Rainfall spatial variability is a crucial factor determining rainfall input in hydrological models and it significantly affects model simulation accuracy. We selected the Yangshudang watershed in the Zhanghe irrigation district of Yangtze River Basin of China to assess the impact of rainfall spatial variability on SWAT runoff simulation in hilly irrigation areas. Eight different rainfall station network distributions were established and rainfall data were processed, using the SWAT model nearest and Thiessen polygon interpolation methods to analyze rainfall spatial variations in the study area. This study investigated the effects of the number, layout, and rainfall grades of rainfall gauges on runoff simulation performance. The results indicated that a higher number of rainfall gauges and more uniform spatial distribution leads to better runoff simulation performance. Among the scenarios examined, using three rainfall gauges yielded the best results, with R<sup>2</sup>, NSE, and RSR values of 0.84, 0.81, and 0.44, respectively. Employing Thiessen polygon interpolation with three rainfall gauges the R<sup>2</sup> value increased to 0.87, enhancing it by 3.57% and further reducing the simulation errors caused by rainfall spatial variability. Additionally, runoff simulation under different rainfall grades exhibited varying responses to rainfall spatial variability, with minimal impact observed during light rainfall and the greatest impact during moderate and heavy rainfall events.

**Keywords:** *SWAT model, rainfall grades, Thiessen polygon interpolation, rainfall station network distributions, simulation accuracy*

## Introduction

Understanding the water cycle and its transformation patterns is of paramount importance for irrigation district water resource management. At the watershed scale, due to the lack of large-scale long-term surface observation data, hydrological modeling is the optimal method for representing irrigation district water cycling processes (Chun-Ling et al., 2006; Xie and Cui, 2011). Among the numerous available hydrological models, the soil and water assessment tool (SWAT) model has been widely applied in irrigation district water cycling studies due to its strong physical basis, in addition to its comprehensive consideration of anthropogenic factors and geographical features (Chen et al., 2020; Luo et al., 2008; Zheng et al., 2010). The hilly rice irrigation areas in the

Yangtze River Basin exhibit distinct topographic characteristics, with numerous water bodies, such as gullies, channels, ponds, and weirs, facilitating frequent water exchanges. These zones feature a typical “melon-on-the-vine” and display irrigation characteristics typical of the combined use of multiple water sources. The “melon-on-the-vine” irrigation system is one of the typical irrigation network system in the hilly regions of southern China. In this type of network, along with water sources and destinations, there are many reservoirs, ponds, and other water storage facilities connected to the canal network. Small watersheds act as the “capillaries” of the primary stem of the Yangtze River Basin, playing a crucial role in water environment pollution control. This is essential for further implementing the protection of the Yangtze River and promoting ecological restoration, with significant practical implications for rural revitalization and the construction of livable, business-friendly areas (Heiner et al., 2015; Zeng et al., 2012).

The SWAT model can adequately consider agricultural management measures and paddy wetland characteristics, rendering it suitable for simulating hydrological processes in typical irrigation areas of the Yangtze River Basin (Engebretsen et al., 2019; Rivas-Tabares, 2019). In the SWAT modeling process, rainfall, as the main input parameter (Koua et al., 2019), plays a decisive role in simulating the production and routing of runoff. However, rainfall input is influenced by various factors, among which the spatial distribution of rainfall is a crucial determinant of rainfall input accuracy and a current research hotspot. The studies by Smith et al. (2009) have illustrated that the efficiency of runoff simulation in a particular area can be enhanced by combining multiple data sources, and that the accuracy of rainfall input largely determines the accuracy of watershed runoff simulation. Dominguez et al. (Dominguez, 2002) investigated the impact of the spatial variability of rainfall on peak flow and runoff simulation, demonstrating that different rainfall spatial variability patterns can produce differences in flow and vary with changes in watershed area. Cho et al. (2009) found, via the study of three different rainfall station input methods, that spatial variations are more important in rainfall than temporal variations and exert a greater impact on changes in runoff, highlighting that accurately characterizing rainfall spatial variability can significantly reduce model simulation uncertainty.

Currently, researchers generally believe that increasing the density of rainfall stations to reduce rainfall spatial variability can significantly improve the simulation accuracy of hydrological models (Haney et al., 2016; Natumanya et al., 2022). In practical applications, rainfall station distribution is often uneven, and interpolation methods are commonly used to interpolate rainfall data for the purpose of mitigating the effects of rainfall spatial variability. Guo et al. (2021) utilized inverse distance weighting (IDW), empirical Bayesian kriging (EBK), and spline methods to interpolate rainfall data in a watershed of the Jinsha River. The results indicated that interpolation errors were smaller when rainfall amounts were larger. Pellicone et al. (2018) applied different spatial interpolation algorithms to rainfall data in southern Italy (Calabria) and compared the results between geostatistical and deterministic methods to select the optimal method for reproducing the actual rainfall surface. Among these methods, the technique of kriging with an external drift exhibited the smallest prediction error. Feng et al. (2017) introduced the nearest method, Thiessen polygon method, inverse distance weighting method, and kriging method for sub-watershed areal rainfall calculation. The results showed that the accuracy of the four interpolation methods was similar. However, the results of the inverse distance weighting and Thiessen polygon methods were more stable.

While there is ample research on rainfall spatial variability, much of it focuses on interpolation methods for model rainfall data, particularly in large study areas with evenly distributed rainfall stations. However, in practical applications, rainfall station placement in small watersheds is often more random, resulting in significant spatial variability in rainfall, with varying degrees of difference among rainfall grades. This is especially true in the hilly irrigation areas of southern China, where there are numerous paddy fields and ponds, the impact of which on runoff is not yet clear. Therefore, this study focuses on the Yangshudang (YSD) watershed in the Zhanghe irrigation district (ZHID) of Yangtze River Basin of China to analyze the impact of different combinations of rainfall stations on runoff simulation. Our research compares the results with those obtained using the Thiessen polygon interpolation method, investigates the effect of rainfall spatial variability on runoff simulation, and assesses the influence of rainfall spatial variability on runoff simulation under different rainfall grades. This research aims to provide insights for optimizing the layout of local rainfall stations and selecting station data.

## Materials and methods

### *Study area*

The study area selected is the YSD watershed in the ZHID of Hubei Province, China, with an area of approximately 40 km<sup>2</sup>. The elevation ranges from below 200 m to over 50 m, with slope inclines mainly concentrated between 2° and 6°, which is typical of hilly terrain. The internal water exchange is complex and frequent, with the exception of the YSD Reservoir at the outlet; there is also a small reservoir, the Honghe Reservoir, within the watershed. The area is relatively enclosed within the ZHID, being surrounded by three main canals. The climate in the study area is classified as subtropical continental, with an average annual temperature of 17°C and a maximum temperature of 40.9°C. The average annual rainfall is around 1000 mm, with uneven spatial distribution, being higher in the south and west compared to the north and east. Rainfall is also unevenly distributed throughout the year, with 85% occurring from April to October, and the period from July to August alone accounting for over one-third of the annual total. The main crops grown in the YSD watershed include rice, cotton, and rapeseed, with rice cultivation predominating, covering about 60% of the total cultivated area, predominantly under intermittent irrigation (Wu et al., 2019). Additionally, there are numerous ponds and weirs in the watershed, with a contributing area ratio of 0.405. The storage capacity of rice fields and weirs causes a significant lag in rainfall runoff within the watershed. The location of the watershed is shown in *Figure 1*. The distribution of land use and soil types in the study area is illustrated in *Figure 2*.

### *Model setup*

The SWAT model requires two types of input data: attribute data and spatial data. Attribute data mainly include meteorological and hydrological observation data. Conversely, meteorological data mostly comprise daily rainfall, maximum temperature, minimum temperature, relative humidity, and average wind speed. These values are taken from the Tuanli Irrigation Experimental Station (referred to as the TL rainfall station), R03 (from experimental observations), and the YSD Reservoir rainfall station

(referred to as the P08 rainfall station) for the years 2020-2022. Hydrological observation data consist of flow monitoring data for the years 2020-2022, sourced from the YSD Reservoir Management Office. Spatial data include digital elevation data (DEM) with a resolution of 12.5 m, land use maps (resolution of 5 m), and soil type maps (resolution of 14.25 m).

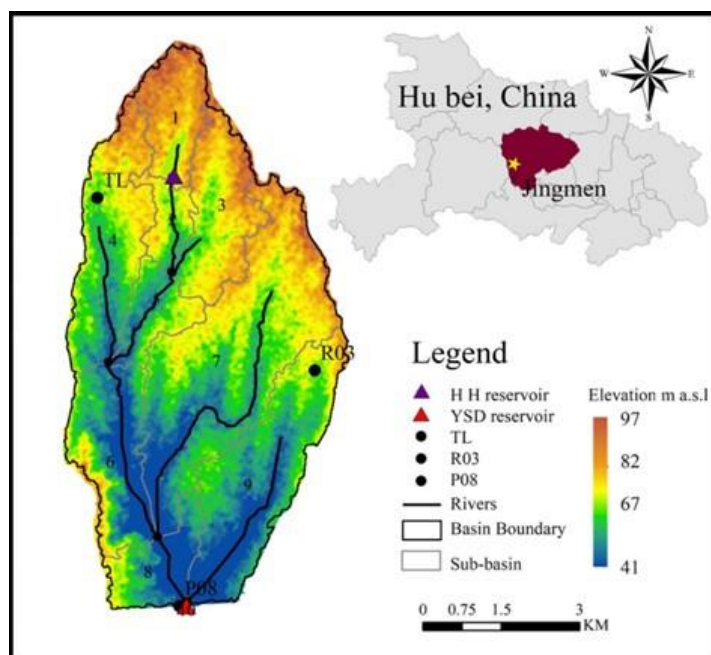


**Figure 1.** The location of study area and sub-basin division (TL, R03 and P08 represent the three rain stations in the study area)

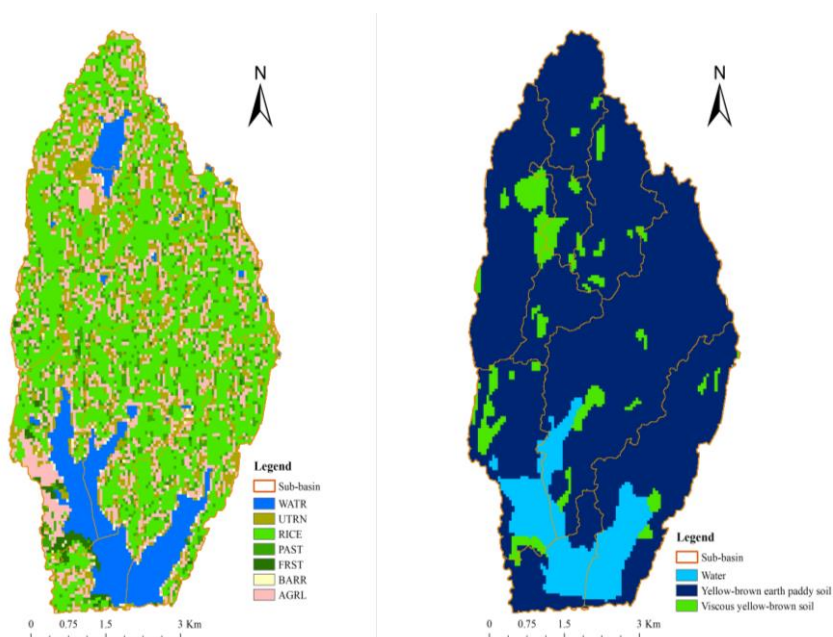


**Figure 2.** Spatial distributions of land use type (UTRN stands for built-up land; PAST stands for grassland; FRST stands for forest land; BARR stands for bare land; and AGRL stands for dry land) and soil type of study area

The SWAT model uses the SCS runoff curve number method to perform runoff simulation. The river network is delineated and corrected based on DEM information and actual water systems, with the outlet of the YSD Reservoir added as the basin outlet, resulting in 10 sub-basins (Fig. 1). Rainfall and meteorological data within each sub-basin are extracted from the nearest station to the centroid of the sub-basin. Sub-basins are divided into hydrological response units (HRUs), with runoff calculated separately for each HRU. Finally, runoff is routed to the basin outlet through flow routing calculations.

### ***Rainfall spatial interpolation algorithm***

Rainfall spatial interpolation can transform discrete rainfall station data in a watershed into a continuous data surface to deduce the rainfall values of other arbitrary points within the range. Two rainfall spatial interpolation algorithms are used in this paper, including the nearest method, which is the default technique of the SWAT model, and the Thiessen polygon method.

#### *Nearest interpolation*

The default rainfall interpolation algorithm in the SWAT model is the nearest interpolation method (Feng et al., 2017). It selects the rainfall value of the first station that falls within a circular area centered at the location requiring interpolation, starting from the circle with the smallest radius (Maletta et al., 2005).

#### *Thiessen polygon interpolation*

The Thiessen polygon method uses the measurement stations located within the watershed as vertices to form several non-nested triangles (Feng et al., 2017; Nguyen and Dietrich, 2018). The perpendicular bisectors of the three sides of each triangle are connected, and the intersection points of these perpendicular bisectors divide the watershed into several polygons. The calculation formula for the average areal rainfall in the area is as follows (Eq. 1):

$$\bar{P} = \frac{1}{A} \sum_{i=1}^n p_i a_i \quad (\text{Eq.1})$$

where  $\bar{P}$  is the regional average areal rainfall, mm;  $A$  is the area of the region, km<sup>2</sup>;  $a_i$  is the area of the  $i$ th Tyson polygon in the region, km<sup>2</sup>;  $p_i$  is the rainfall data of the station which corresponds to the  $i$ th Tyson polygon, mm; and  $i$  ranges from 1 to the total number of Thiessen polygons in the region.

### ***Model evaluation metrics***

Runoff simulation results are evaluated using  $R^2$  (coefficient of determination), NSE (Nash coefficient), RSR (the ratio of the Nash coefficient, root-mean-square deviation, and standard deviation), which is used to analyze the impact of different rainfall spatial variations on the runoff simulation.  $R^2$  represents the consistency between observed data and simulated data. NSE is used to measure the fitting degree between observed and simulated data. RSR is utilized to standardize the root-mean-square error, and the

smaller the absolute value of RSR, the better the simulation performance of the model (Zhang et al., 2008). The calculation formula for each evaluation indicator is as follows (Eqs. 2–4):

$$R^2 = \frac{[\sum_{i=1}^n (Q_{obs,i} - \bar{Q}_{obs})(Q_{sim,i} - \bar{Q}_{sim})]^2}{\sum_{i=1}^n (Q_{obs,i} - \bar{Q}_{obs})^2 \sum_{i=1}^n (Q_{sim,i} - \bar{Q}_{sim})^2} \quad (\text{Eq.2})$$

$$NSE = 1 - \frac{\sum_{i=1}^n (Q_{obs,i} - \bar{Q}_{sim,i})^2}{\sum_{i=1}^n (Q_{obs,i} - \bar{Q}_{obs})^2} \quad (\text{Eq.3})$$

$$RSR = \frac{\sqrt{\sum_{i=1}^n (Q_{obs,i} - \bar{Q}_{sim,i})^2}}{\sqrt{\sum_{i=1}^n (Q_{obs,i} - \bar{Q}_{obs})^2}} \quad (\text{Eq.4})$$

where  $Q_{obs,i}$  is the observed value;  $Q_{sim,i}$  is the simulated value;  $\bar{Q}_{obs}$  is the average of all observed values;  $\bar{Q}_{sim}$  is the average of all simulated values; and  $n$  is the number of the observed data. Generally, when RSR is less than 0.7, and  $R^2$  and NSE are greater than 0.6 and 0.5 respectively, the model simulation results are considered to be more reliable.

### Schematic

We combined three rainfall stations in eight different scenarios, as shown in *Table 1*. Runoff simulations were performed using the nearest method and the Thiessen polygon interpolation method, respectively. The interpolation results are shown in *Figure 3* and *Table 2*.

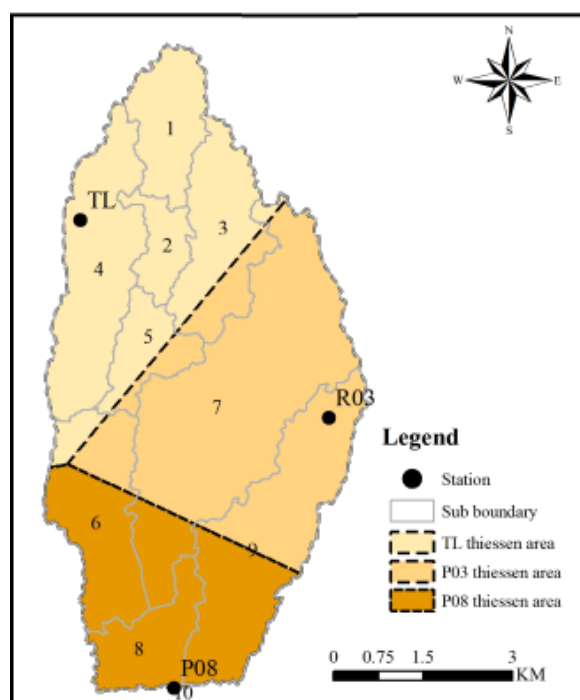


**Figure 3.** Tyson polygon interpolation results

**Table 1.** Rainfall station selection scenario setting scheme

Scenarios	Number of rainfall measuring stations	Selection of rainfall stations	Sub-basin		
			TL	R03	P08
S1	1	R03	/	1-10	/
S2	1	P08	/	/	1-10
S3	1	TL	1-10	/	/
S4	2	TL + P08	1-5, 7	/	6, 8-10
S5	2	P08 + R03	/	1-7, 9	8, 10
S6	2	TL + R03	1-5	6-10	/
S7	3	TL + R03 + P08	1-5	6, 7, 9	8, 10
S8	3	TL + R03 + P08 (Thiessen polygon method)	/	/	/

**Table 2.** Tyson polygon weight calculation

Sub-basin	Proportion of weight of each rainfall station		
	TL	R03	P08
1	1.000	/	/
2	1.000	/	/
3	0.640	0.360	/
4	1.000	/	/
5	0.666	0.334	/
6	0.169	0.22	0.611
7	0.004	0.887	0.109
8	1.000	/	/
9	/	0.576	0.424
10	1.000	/	/

## Results and discussion

### *Analysis of rainfall spatial variability*

The daily rainfall data from three rainfall stations in the YSD watershed were analyzed, and the results are shown in *Figure 4*. The daily rainfall ranges measured at three rainfall stations were 0.3-92 mm, 0.2-49.8 mm and 0.5-67.5 mm, and the average daily rainfall values were 12.5 mm, 9.2 mm, and 12.96 mm, respectively. The results showed that, although the area of YSD watershed was not large, there remained significant differences in daily rainfall at the level of spatial distribution. Thus, it was necessary to study the impact of rainfall spatial variability on runoff simulation.

### *Impact of rainfall spatial variability on daily runoff simulation*

Different combinations of rainfall stations were employed to determine rainfall input. The model was preheated using data from 2020. Calibration and validation were conducted using daily runoff data from the YSD outlet for May to September of 2021 and 2022, respectively. The runoff simulations were analyzed in order to evaluate the performance of each scheme, with results summarized in *Table 3*.

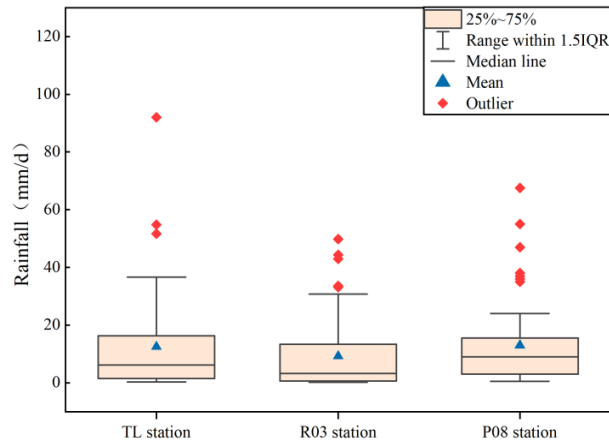


**Figure 4.** Comparison of rainfall data from different gauging stations

**Table 3.** Comparison of simulation effects of different scenarios

Scenarios	Combinations of rainfall stations	R <sup>2</sup>	NSE	RSR
S1	R03	0.54	0.48	0.72
S2	P08	0.55	0.39	0.76
S3	TL	0.55	0.27	1.13
S4	TL + P08	0.69	0.49	0.72
S5	P08 + R03	0.57	0.51	0.70
S6	TL + R03	0.82	0.79	0.46
S7	TL + R03 + P08	0.84	0.81	0.44
S8	TL + R03 + P08(TS)	0.87	0.81	0.44

The results in *Table 3* illustrate that both the number and layout of rainfall stations influence the results of the simulation. For individual rainfall stations, the R<sup>2</sup> and NSE values for schemes S1, S2, and S3 are all below 0.6, with RSR values exceeding 0.7. With two rainfall stations, schemes S4, S5, and S6 exhibit better simulation performances compared to S1, S2, and S3. The R<sup>2</sup> values range from 0.57 to 0.82, NSE values range from 0.49 to 0.79, and RSR values range from 0.46 to 0.72. In the case of three rainfall stations, schemes S7 and S8 demonstrate the best simulation results, with R<sup>2</sup> and NSE values both exceeding 0.8 and with RSR values below 0.5, indicating a robust level of accuracy (Sime et al., 2022). It is evident that, as the number of rainfall stations increases, the simulation performance gradually improves, with noticeable differences visible, underscoring the significant impact of the number of rainfall stations on simulation results.

Furthermore, under the scenarios using two rainfall station combinations (S4 and S5), the R<sup>2</sup> and NSE are below 0.7, with RSR reaching 0.7. Conversely, for scenario S6, the R<sup>2</sup> and NSE values are 0.82 and 0.79, respectively, with RSR standing at merely 0.46. This suggests that different combinations of rainfall stations exert a certain influence on simulation results, with scenario S6 showing better performance. According to *Table 1*, the usage of rainfall station data by model sub-basins reveals that scenario S4 ignores rainfall data in the central region by utilizing upstream and downstream rainfall stations, while scenario S5 disregards rainfall in the upper basin by



allocating 80% of sub-basins to the downstream R03 and 20% to the downstream P08. Consequently, the simulation performance of S4 and S5 scenarios is inferior. In contrast, scenario S6 features a more uniform distribution of rainfall stations, which can represent both higher- and lower-elevation areas, leading to a relatively reasonable allocation of rainfall stations by sub-basin and the best simulation results. This indicates that the accuracy of runoff simulation is also influenced by the layout of rainfall stations, with a more evenly distributed network resulting in better simulation performance (Li et al., 2024). This finding aligns with the results of Zhang et al. (Zhang, 2018), who conducted an analysis of differences in basin runoff processes under various rainfall station network densities and spatial distribution patterns in the Chaba River basin. This result also concurs with the research of Zeng et al. (2018), who used the Xin'anjiang model to assess the impact of rainfall gauge density and distribution on the uncertainty of comprehensive hydrological models under different basin scales.

Among all scenarios, schemes S7 and S8 demonstrate the best simulation performance, with all evaluation indicators reaching a strong level. Both schemes utilize the same rainfall station data, but the simulation performance of S8 is slightly higher than that of S7, indicating that employing the Thiessen polygon interpolation method, which considers the influence between rainfall stations, can further reduce the error impact of rainfall spatial variability on runoff simulation (Lisboa et al., 2024). However, the improvement in effectiveness is marginal.

### ***Impact of rainfall spatial variability on runoff simulation under different rainfall grades***

For the purpose of analyzing the impact of rainfall spatial variability on runoff under different rainfall grades, rainfall events detected by stations during the growing season were classified into four grades (light rainfall, moderate rainfall, heavy rainfall, and rainstorm) according to the standard (GB/T 28592-2012) issued by the National Meteorological Bureau (Zhang et al., 2022), as presented in Table 4. Their proportions are shown in Figure 5. Figure 5 shows that the YSD watershed mainly experienced light rain, followed by moderate and heavy rain, during the experimental periods. Runoff simulation results under different rainfall grades are shown in Table 5.

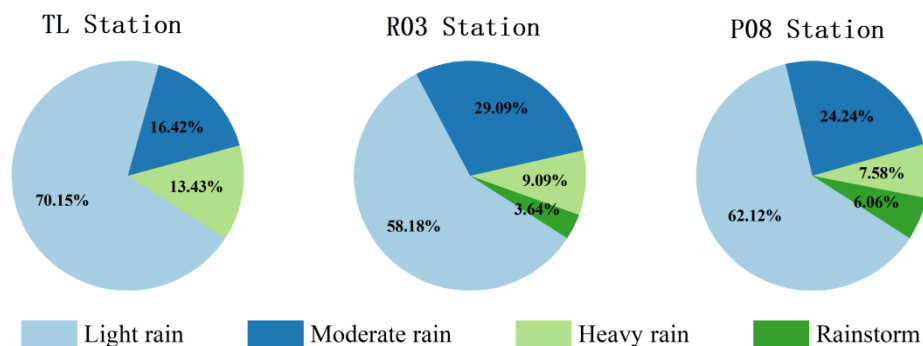


***Figure 5.*** The proportion of rainfall grade in different rainfall measuring stations

Based on Table 5, it is evident that, under light rainfall conditions, most simulation outcomes for schemes S1-S8 are satisfactory. In such circumstances, the majority of R<sup>2</sup>

values exceed 0.7, NSE ranges from 0.62 to 0.84, and the absolute values of RSR are mostly below 0.6. However, when rainfall intensity increases to moderate or heavy grades, simulation performance notably declines: for S1-S7 schemes, most  $R^2$  values are below 0.7, NSE values are all less than 0.7, and the absolute values of RSR mostly exceed 0.9, indicating poor simulation results. Only under scheme S8 do results meet the model's applicability criteria, with an  $R^2$  of 0.7, NSE of 0.6, and an absolute value of RSR below 0.6. In the case of heavy rainfall, while most  $R^2$  values under schemes S1-S8 reach 0.8, NSE and RSR results indicators are poor, indicating a consistent trend with observed results but with low fitting accuracy and reasonably large relative errors.

**Table 4.** Rainfall grades

Grades	24-h rainfall (mm)
Light rainfall	0.1~9.9
Moderate rainfall	10.0~24.9
Heavy rainfall	25.0~49.9
Rainstorm	$\geq 50.0$

**Table 5.** Simulation effect of different scenarios under different rainfall grades

	Light rainfall			Moderate rainfall			Heavy rainfall			Rainstorm		
	$R^2$	NSE	RSR	$R^2$	NSE	RSR	$R^2$	NSE	RSR	$R^2$	NSE	RSR
S1	0.68	0.62	0.62	0.36	0.04	0.98	0.08	-0.07	1.04	0.9	-0.45	1.21
S2	0.69	0.61	0.63	0.53	0.12	0.76	0.44	0.12	0.88	0.33	-0.32	1.31
S3	0.68	0.62	0.69	0.52	-1.08	1.44	0.58	-2.07	1.75	0.21	-2.31	1.82
S4	0.85	0.82	0.42	0.65	0.11	0.94	0.64	0.21	1.1	0.01	-0.91	1.38
S5	0.71	0.65	0.59	0.41	0.13	0.93	0.13	-0.03	1.01	0.9	-0.41	1.19
S6	0.81	0.79	0.46	0.1	-4.41	2.33	0.7	0.65	0.59	0.82	-0.24	1.11
S7	0.83	0.81	0.43	0.67	0.63	0.61	0.74	0.69	0.56	0.83	-0.18	1.09
S8	0.87	0.84	0.39	0.73	0.66	0.59	0.85	0.68	0.57	0.82	-0.38	1.17

From the perspective of rainfall spatial variability, as rainfall intensity increases, the influence of spatial variability on simulation outcomes also increases (Assani, 2024; Lisboa et al., 2024): under light rainfall conditions, the difference in individual evaluation indicators among schemes S1-S8 does not exceed 0.3. However, when rainfall intensity shifts to moderate or heavy grades, the maximum difference in individual indicators can reach 5.07. For heavy rainfall, only some schemes exhibit solid  $R^2$  values, while the rest of the indicators are poor.

The model has minimal impact on runoff simulation under light rainfall, primarily due to the small amount of rainfall and limited influence of rainfall spatial variability (Ali et al., 2024). Rainfall spatial variability exercises a significant impact on runoff simulation under moderate and heavy rainfall, but there is no obvious pattern. Runoff simulation consistency is better under heavy-rainfall conditions, but both fitting accuracy and error are poor. This is primarily due to the frequent occurrence of short, moderately sized, and single-peak storms in the YSD watershed, where runoff hysteresis is evident and subject to high spatial variability (Jin et al., 2008).

In the practical rainfall station layout, if the study area experiences predominantly light rainfall, reducing the number of rainfall stations appropriately can help to cut costs. Conversely, if the area experiences moderate or heavy rainfall, increasing the density of rainfall stations is advisable to achieve better simulation results. Moreover, if heavy rainfall events are common in the study area, attention should be paid to the fitting of runoff simulation and relative errors during the modeling process.

## Conclusions

This study takes the YSD watershed in the ZHID as an example in order to analyze the runoff simulation effects under different combinations of rainfall stations and different rainfall intensities using the SWAT model, aiming to reveal the influence of rainfall spatial variability on runoff simulation. The primary conclusions are summarized below.

The number of rainfall stations significantly affects the accuracy of runoff simulation. The worst simulation results are obtained under the scenario of using only the R03 rainfall station, with  $R^2$ , NSE, and RSR values of 0.54, 0.48, and 0.72, respectively. As the number of rainfall stations increases, the accuracy of the simulation continuously improves, with the best simulation results obtained using three rainfall stations, with  $R^2$ , NSE, and RSR values of 0.84, 0.81, and 0.44, respectively. This indicates that increasing the number of rainfall stations can significantly improve the simulation accuracy. Compared to the scenario with three rainfall stations, using the Thiessen polygon interpolation method only increased the  $R^2$  indicator by 3.57%. This suggests that using interpolation methods in this basin can indeed improve simulation accuracy, but that the enhancement is limited.

The accuracy of runoff simulation is not only influenced by the number of rainfall stations but also by the distribution of rainfall station networks. Under the same number of rainfall stations in the basin, a reasonable distribution of rainfall stations can increase simulation accuracy by 40%. Therefore, when deploying rainfall stations in the basin, stations should be evenly distributed.

The smaller the rainfall intensity in the basin, the less of an impact rainfall spatial variability has on runoff simulation, and the better the simulation results. Under different scenarios, the difference in simulation effects for light rainfall is minimal, and all results meet the applicability of the model; for moderate and heavy rain, only 28.57% of results can meet the applicability of the model, and the differences in simulation results are significant; finally, the simulation effect of heavy rainfall is the worst and cannot meet the requirements of the model evaluation.

Due to the relatively short number of years of experimentation in the study area, this study only analyzed data from 2021 to 2022, using a short time series. Consequently, further exploration is needed for long-term series patterns. Only three rainfall stations within the study area were used in this research, and the impact of rainfall station combinations can be further analyzed by adding a greater number of rainfall stations in the future.

**Acknowledgements.** The National Natural Science Foundation of China-the Ministry of Water Resources of the People's Republic of China-China Yangtze River Three Gorges Group Co., Ltd. Yangtze River Water Science Research Joint Fund Project (No. U2040213), the basic scientific research business funding projects of central public welfare research institutes (CKSF2019251/NY, CKSF2021299/NY) and Knowledge Innovation Program of Wuhan-Shuguang Project (2023020201020362).

## REFERENCES

- [1] Ali, G., Siebert, K., Mizero, S. M. (2024): Spatiotemporal variability of runoff events in response to rainfall, snowmelt, and rain-on-snow in the Lake Erie Basin. – *Journal of Hydrology: Regional Studies* 53:101774. <https://doi.org/10.1016/j.ejrh.2024.101774>.
- [2] Assani, A. A. (2024): Analysis of the impacts of climate change, physiographic factors and land use/cover on the spatiotemporal variability of seasonal daily mean flows in southern Quebec (Canada). – *Applied Water Science* 14: 109.
- [3] Chen, Y., Marek, G. W., Marek, T. H., Porter, D. O., Moorhead, J. E., Heflin, K. R., Brauer, D. K., Srinivasan, R. (2020): Watershed scale evaluation of an improved SWAT auto-irrigation function. – *Environmental Modelling & Software* 131. <https://doi.org/10.1016/j.envsoft.2020.104789>.
- [4] Cho, J., Bosch, D., Lowrance, R., Strickland, T., Vellidis, G. (2009): Effect of spatial distribution of rainfall on temporal and spatial uncertainty of SWAT output. – *Transactions of the Asabe* 52: 1545-1556.
- [5] Chun-Ling, L., Yan-Fen, W., Shi-Hu, Z., Lian-Yao, Z. (2006): Realization of embedded telemetering system of hydrological signal based on ARM for irrigation district. – *Water Resources and Hydropower Engineering* 8: 74-77
- [6] Dominguez, C. R. (2002): Influence of rainfall spatial variability on flood prediction. – *Journal of Hydrology*. [https://doi.org/10.1016/S0022-1694\(01\)00611-4](https://doi.org/10.1016/S0022-1694(01)00611-4).
- [7] Engebretsen, A., Vogt, R. D., Bechmann, M. (2019): SWAT model uncertainties and cumulative probability for decreased phosphorus loading by agricultural Best Management Practices. – *Catena* 175: 154-166.
- [8] Feng, X., Peng, S., Jian-Wei, H. U., Si-Min, Q. U., Yan-Ming, Z., Man-Man, L. I., Zhi-Gang, X. (2017): Study on effect of uncertainty in spatial distribution of rainfall on runoff modeling based on SWAT model. – *China Rural Water and Hydropower* 10: 23 -27.
- [9] Guo, X., Cui, P., Chen, X., Li, Y., Zhang, J., Sun, Y. (2021): Spatial uncertainty of rainfall and its impact on hydrological hazard forecasting in a small semiarid mountainous watershed. – *Journal of Hydrology* 595. <https://doi.org/10.1016/j.jhydrol.2021.126049>.
- [10] Haney, E. B., Haney, R. L., Arnold, J. G., White, M. J., Senseman, S. A. (2016): Spatial analysis and modeling the nitrogen flush after rainfall events at the field scale in SWAT. – *American Journal of Environmental Sciences* 12(2): 102-121.
- [11] Heiner, M., Higgins, J., Xinhai, L. I., Baker, B. (2015): Identifying freshwater conservation priorities in the Upper Yangtze River Basin. – *Freshwater Biology* 56: 89-105.
- [12] Jin, X., Guangcheng, H. U., Wenmei, L. I. (2008): Hysteresis effect of runoff of the Heihe River on vegetation cover in the Ejina Oasis in Northwestern China. – *Earth Science Frontiers* 15: 198-203.
- [13] Koua, T., Kouassi, H., Anoh, K. (2019): Analysis of the SWAT (soil and water assessment tool) semi-distributed model input data for the hydrological simulation of the Lobo Water Reservoir (Central West of Cote d'Ivoire). – *Journal of Geography, Environment and Earth Science International*. DOI: 10.9734/jgeesi/2019/v23i430182.
- [14] Li, W., Li, Y., Xin, J., Huang, H. (2024): The effect of interfacial strength on the mesoscopic damage characteristics of resin-mineral composite based on PFC3D. – *Computational Particle Mechanics* 11: 853-865.
- [15] Lisboa, A. E. A., Fazzioni, P. F. P. C., Chinelli, C. K., Faisca, R. G., Soares, C. A. P. (2024): Influence of the accumulated precipitation and the spatial distribution of rainfall on the results of reservoir sizing methodologies. – *International Journal of Environmental Science and Technology* 21: 5149-5164.
- [16] Luo, Y., He, C., Sophocleous, M., Yin, Z., Hongrui, R., Ouyang, Z. (2008): Assessment of crop growth and soil water modules in SWAT2000 using extensive field experiment

- data in an irrigation district of the Yellow River Basin. – *Journal of Hydrology* 352: 139-156.
- [17] Maletta, R., Huisman, J. A., Breuer, L., Frede, H. G., Mendicino, G. (2005): Impact of precipitation data interpolation on the quality of SWAT simulation. – In: Third International SWAT Conference, July 11-15, Zürich.
- [18] Natumanya, E., Ribeiro, N., Mwanjalolo, M. J. G., Steinbruch, F. (2022): Using SWAT model and field data to determine potential of NASA-POWER data for modelling rainfall-runoff in Incalaue River Basin. – *Computational Water, Energy, and Environmental* 11. DOI: 10.4236/cweee.2022.112004.
- [19] Nguyen, V. T., Dietrich, J. (2018): Modification of the SWAT model to simulate regional groundwater flow using a multicell aquifer. – *Hydrological Processes* 32: 939-953.
- [20] Pellicone, G., Caloiero, T., Modica, G., Guagliardi, I. (2018): Application of several spatial interpolation techniques to monthly rainfall data in the Calabria region (southern Italy). – *International Journal of Climatology: A Journal of the Royal Meteorological Society* 38: 3651-3666.
- [21] Rivas-Tabares, D., Tarquis, A. M., Willaarts, B., De Miguel, A. (2019): An accurate evaluation of water availability in sub-arid Mediterranean watersheds through SWAT: Cega-Eresma-Adaja. – *Agricultural Water Management* 212. <https://doi.org/10.1016/j.agwat.2018.09.012>.
- [22] Sime, C. H., Abebe, W. T., Senapathi, V. (2022): Sediment yield modeling and mapping of the spatial distribution of soil erosion-prone areas. – *Applied and Environmental soil Science*. DOI: 10.1155/2022/4291699.
- [23] Smith, M. B., Koren, V. I., Zhang, Z., Reed, S. M., Pan, J. J., Moreda, F. (2009): Runoff response to spatial variability in precipitation: an analysis of observed data. – *Journal of Hydrology* 370: 139-154.
- [24] Wu, D., Cui, Y., Wang, Y., Chen, M., Luo, Y., Zhang, L. (2019): Reuse of return flows and its scale effect in irrigation systems based on modified SWAT model. – *Agricultural Water Management* 213. <https://doi.org/10.1016/j.agwat.2018.10.025>.
- [25] Xie, X., Cui, Y. (2011): Development and test of SWAT for modeling hydrological processes in irrigation districts with paddy rice. – *Journal of Hydrology* 396: 61-71.
- [26] Zeng, Q., Chen, H., Chong-Yu, X., Jie, M., Chen, J., Guo, S., Liu, J. (2018): The effect of rain gauge density and distribution on runoff simulation using a lumped hydrological modelling approach. – *Journal of Hydrology* 563: 106-122.
- [27] Zeng, X., Kundzewicz, Z. W., Zhou, J., Su, B. (2012): Discharge projection in the Yangtze River basin under different emission scenarios based on the artificial neural networks. – *Quaternary International* 282: 113-121.
- [28] Zhang, L. (2018): Study on dynamic warning and risk assessment method for mountain torrents in small watershed. – PhD Thesis, Zhengzhou University.
- [29] Zhang, P., Chen, L., Yan, T., Liu, J., Shen, Z. (2022): Sources of nitrate nitrogen in urban runoff over and during rainfall events with different grades. – *Science of the Total Environment* 808: 152069.
- [30] Zhang, X., Srinivasan, R., Debele, B., Hao, F. (2008): Runoff simulation of the headwaters of the Yellow River Using the SWAT model with three snowmelt algorithms. – *JAWRA Journal of the American Water Resources Association* 44(1): 48-61
- [31] Zheng, J., Li, G., Han, Z., Meng, G. (2010): Hydrological cycle simulation of an irrigation district based on a SWAT model. – *Mathematical & Computer Modelling An International Journal* 51: 1312-1318.